

Chapter

NUMERICAL MODELING OF RECRYSTALLIZATION IN A LEVEL SET FINITE ELEMENT FRAMEWORK FOR APPLICATION TO INDUSTRIAL PROCESSES

M. Bernacki¹, N. Bozzolo¹, P. de Micheli², B. Flipon¹, J. Fausty¹, L. Maire¹, S. Florez¹

¹MINES ParisTech, PSL Research University, CEMEF – Centre de mise en forme des matériaux, CNRS UMR 7635, CS 10207 rue Claude Daunesse, Sophia Antipolis Cedex 06904, France

²TRANSVALOR S.A., E-Golf Park, 950 Avenue Roumanille, 06410 Biot, France

ABSTRACT

Recently, an original full field model working at the mesoscopic scale using the level set (LS) method in a finite element (FE) framework has been introduced. This approach has demonstrated its potential for the simulation of grain growth and recrystallization problems in the context of large deformations, allowing its use for industrial thermomechanical paths. This chapter illustrates the basis of this numerical framework, its evolutions since 20 years and very recent developments.

Keywords: Recrystallization, Grain Growth, Full Field Methods, Level Set Approach, Industrial Processes

INTRODUCTION

Metal forming modeling can be predictive only if the strain rate, strain and temperature dependency of the flow behaviour are correctly described. The mechanical properties and behaviour of metallic materials mainly depend on the density and structure of dislocation network, this points out the need of

incorporating microstructure concepts into the numerical models. On the other hand, mastering grain size and dislocation density evolutions due to recrystallization (ReX) during industrial processes becomes necessary to fulfill more and more severe microstructure and properties specifications of the processed materials. This objective implies to correctly describe the main physical mechanisms occurring in metals during thermomechanical processing, notably *dynamic recrystallization* (DRX), *postdynamic recrystallization* (PDRX) - possibly including *metadynamic recrystallization* (MDRX) and *static recrystallization* (SRX) mechanisms - and *grain growth* (GG).

However, microstructure predictions on multi-pass processes are very challenging due to the strong evolution of the microstructure topology from the beginning to the end of the process. The competition between boundary migration, recovery and nucleation leads to complex coupled effects. Minor variations of the process parameters (interpass and/or reheating times, temperature and strain rate values at each pass) may have huge effects on the way DRX and PDRX take place.

In this context, macroscopic and homogenized models, *i.e. phenomenological models* such as those based on the well-known Johnson-Mehl-Avrami-Kolmogorov (JMAK) equations (Avrami 1939; Kolmogorov 1937; Johnson and Mehl 1939) are widely used in the industry, mainly owing to their low computational cost. If this phenomenological framework is quite convenient, the validity range of these models, associated with a given set of material parameters is often limited to a given process and initial material state. To push these limits, *mean field (MF) models*, based on an implicit description of the microstructure by considering grains as spherical entities with an equivalent grain radius and/or an average dislocation density have been developed. Hillert (Hillert 1965) proposed the first model of this kind for GG. Then, Montheillet et al. (Montheillet, Lurdos, and Damamme 2009) and Cram (Cram et al. 2009) proposed a semi-analytical MF model for ReX. More recently, new MF models, proposing, in their formulation, richer description of the neighborhood of each grain have been proposed in order to improve the prediction of grain size distributions (Bernard et al. 2011; Beltran, Huang, and Logé 2015; Zouari, Bozzolo, and Logé 2016; Maire et al. 2018; Piot et al. 2018). Indeed, MF models generally provide acceptable predictions in terms of recrystallization kinetics and mean grain size evolution with very interesting computational cost. However, grain size distributions sourced from MF simulations are sometimes poorly described. Facing multi-pass processes, they rapidly reach their limits. Finally, the homogenization of the microstructure may prevent from capturing some local phenomena.

In order to overcome these issues, lower-scale models (called full field -FF- models) have been developed over the last decades with the aim to simulate

explicitly the microstructural evolution (Rollett and Raabe 2001; Piękoś et al. 2008; Chen 2002) and then to propose *enhanced mean-field models* (Maire et al. 2017; Scholtes, Ilin, et al. 2016). The idea behind these “mesoscale” simulations is that the morphology and the topology of the GB network play an essential role in microstructure evolution. In these approaches, simulations are performed on Representative Volume Elements (RVEs) where the microstructural features are explicitly represented. Boundary conditions applied to the RVE are representative of what suffered a material point at the macroscopic scale (thermal or thermomechanical cycle).

In a full field context, simulations can be performed using probabilistic *Monte Carlo Potts* (MC) (Rollett et al. 1989; Radhakrishnan, Sarma, and Zacharia 1998, 2008; L. Zhang et al. 2012; Wang et al. 2014), *Cellular Automata* (CA) (Raabe 2002; Janssens 2010; Sieradzki and Madej 2013), *MultiPhase Field* (MPF) (Garcke, Nestler, and Stoth 1999; Moelans, Blanpain, and Wollants 2005; Esedoğlu 2016), *Front-Tracking or Vertex* (Harun et al. 2006; Couturier, Maurice, and Fortunier 2003) or *Level Set* (LS) models (Osher and Sethian 1988; Merriman, Bence, and Osher 1994; Zhao et al. 1996; Bernacki et al. 2007, 2008; Bernacki, Logé, and Coupez 2011; Jin et al. 2015; Scholtes, Boulais-Sinou, et al. 2016; Maire et al. 2017; Hallberg 2013; Elsey, Esedoğlu, and Smereka 2009, 2010; Mießen et al. 2015; Bernacki et al. 2009; Resk et al. 2009; Logé et al. 2010). These numerical methods are currently used and developed by many researchers (J. Humphreys, Rohrer, and Rollett 2017) and regularly compared for particular metallurgical mechanisms (Harun et al. 2006; Jin et al. 2015).

Of course, all the mentioned models have their own strengths and weaknesses. Probabilistic voxel-based approaches such as MC and some CA formulations are very popular. These models consider uniform grids composed of cells to model microstructure and stochastic laws to predict the motion of interfaces. These simulations are efficient in term of computational cost and the scalability is excellent. On the other hand, deterministic approaches, based on the resolution of partial differential equations, are more accurate in the description of the involved physical mechanisms although they are numerically more expensive. For instance, front-tracking or vertex approaches are based on an explicit description of interfaces in terms of vertices. Interfaces motion is imposed at each increment by computing the velocity of a set of points. A major difficulty of these approaches is related to the complexity of handling all the possible topological events, such as disappearance and appearance of new grains, which is not straightforward especially in 3D. Other deterministic approaches, also called *front-capturing approaches*, avoid these topological problems since they are based on an implicit description of the interfaces: the MPF and the LS methods. The major limitation of

these two methods is generally the computational cost when used in a finite element (FE) framework.

LS simulations in context of regular grids and Fourier transform resolution, with very large number of grains, can be found for grain growth (Elsey, Esedoğlu, and Smereka 2009; Mießen et al. 2015) and for static recrystallization (Elsey, Esedoğlu, and Smereka 2010) modeling. When global or local meshing/remeshing operations have to be considered (large deformation, presence of second phase particles...), LS approach in context of unstructured finite element (FE) mesh, and reasonable number of grains can be considered (Logé et al. 2008; Bernacki et al. 2008; Bernacki, Logé, and Coupez 2011; Hallberg 2013; Scholtes, Boulais-Sinou, et al. 2016; Maire et al. 2017). This explains the limited number of studies dedicated to the full field modeling of ReX in context of industrial hot metal forming. Indeed, the full field modeling of real thermomechanical paths generally implies to take into account all the concomitant physical mechanisms in context of large or very large deformations.

In the following will be described how the FE-LS method was developed in the last twenty years in this context. First, the LS methodology in context of polycrystals will be briefly recalled. Second, algorithms for modeling ReX and GG in unstructured FE mesh will be described. Discussions concerning the anisotropy of grain boundary energy and how to take into account second phase particles will be illustrated. Then, a typical procedure coming from an industrial thermomechanical path to the use of FE-LS to predict locally grain boundary migration will be described. Finally some current developments of the approach will be discussed.

LEVEL-SET DESCRIPTION OF POLYCRYSTALS

digital microstructure

The LS method was introduced for the first time in 1988 (Osher and Sethian 1988) as a numerical tool to trace the spatial and temporal evolution of interfaces. Several authors have extended this method to interfaces with multiple junctions (Merriman, Bence, and Osher 1994; Zhao et al. 1996) and a first finite element LS framework (FE-LS) for modeling of SRX mechanism in metal alloys was proposed ten years ago (Bernacki et al. 2008; Logé et al. 2008; Bernacki et al. 2009; Resk et al. 2009). In the LS approach, each sub-domain G (grain) in a given domain Ω (polycrystal) is classically described implicitly by computing the signed distance function $\psi(x, t)$ representing the distance to the sub-domain boundaries $\Gamma = \partial G$ (grain boundaries). In a P1 formulation, the function $\psi(x, t)$ is calculated at each

node on the FE mesh and is classically chosen, by convention, positive inside of the grain and negative outside as illustrated in the Figure 1:

$$\forall t \begin{cases} \psi(x, t) = \pm d(x, \Gamma(t)), x \in \Omega \\ \Gamma(t) = \{x \in \Omega, \psi(x, t) = 0\} \end{cases} \quad (1)$$

where $d(\dots)$ corresponds to the Euclidean distance. The interface is implicitly given by the level 0 of the function ψ .

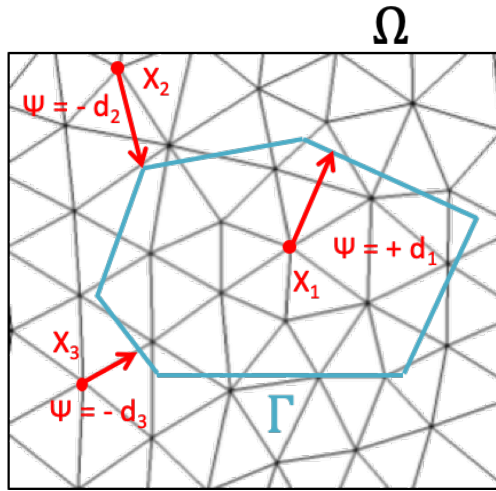


Figure 1. LS description of a polyhedral grain (blue interface) in an unstructured FE mesh (in black).

Using such an implicit description of the interfaces simplifies the definition of the FE mesh as it has not to be correlated to the grain boundary interfaces. Experimental image can be easily immersed in the FE mesh by calculating the distance functions to the grey levels of each grain interface as illustrated in Fig. 2.

When only statistical data are known such as the mean grain size or the grain size distribution, digital material must be built thanks to representative microstructures (Rollett 2004). Voronoï or Laguerre-Voronoï tessellations can be used in order to respect the known data in the generated digital polycrystal made of polyhedral grains. Voronoï Tessellation Method (VTM) consists in generating randomly N Voronoï nuclei and defining each Voronoï cell as the region consisting of all locations in the space which are closer to the considered nucleus than any other nucleus. Despite the good geometric correlation between Voronoï tessellations and many cellular structures, VTM presents some limitations due to the impossibility to respect, for example, a given statistical volume distribution of

cells. Xu and Li (Xu and Li 2009) described the divergence between statistical properties of grains classically observed in an equiaxial polycrystal and results obtained with the VTM. One way to improve the classical VTM consists in using the so-called Laguerre–Voronoi Tessellation Method (LVTM), by assigning a radius, or weight, to each nucleus and to respect this distribution in the Voronoi Tessellation (Imai, Iri, and Murota 1985). It is important to highlight, that the principal difficulty of LVTM is common to the generation of polycrystal microstructure and of powder RVEs: to respect a given statistical size of spheres with the highest possible density. If this criterion seems natural for powder RVEs, it is also crucial for LVTM in order to limit the heterogeneities between the weight imposed and the volume of Voronoi cells finally obtained. This discussion is classically unclear in the literature but put in another way, respecting the grain size distribution for the Laguerre-Voronoi sphere packing is not the same thing that respecting the grain size distribution for the resulting Laguerre-Voronoi cells. Different approaches, gathered in the so-called Sphere Packing Methods (SPM), were developed since 40 years (Jodrey 1985; He, Ekere, and Cai 1999; Lochmann, Oger, and Stoyan 2006; Benabbou et al. 2009; Kansal, Torquato, and Stillinger 2002; Bagi 2005; Cui and O’Sullivan 2003; Bagi 1993; Shi and Zhang 2008) and are classically divided in two families: the sequential addition models and the collective rearrangement ones. Both are intensively developed nowadays for polycrystal generation (Hitti et al. 2012; Ilin and Bernacki 2016b, 2016a; Quey and Renversade 2018; Depriester and Kubler 2019).

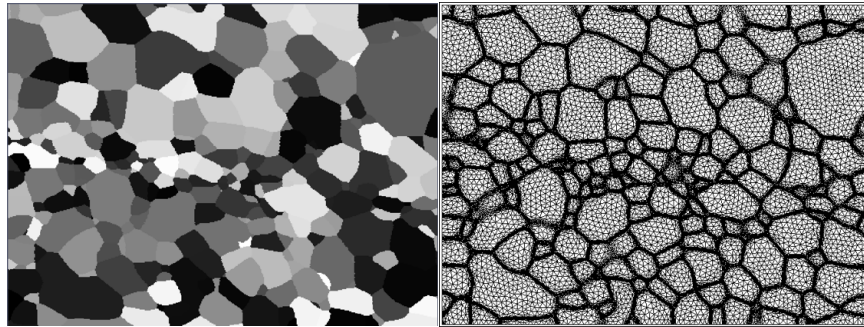


Figure 2. (left) 2D micrograph obtained by EBSD (each grain being plotted with a different gray level) and (right) immersion of the experimental micrograph in a FE mesh thanks to a LS strategy and adaptive anisotropic remeshing around the grain boundaries.

Interestingly, both Voronoi or Laguerre-Voronoi tessellation can be directly described analytically in FE-LS framework thanks to, respectively, Eq. (2) and Eq.

(3) where N_G corresponds to the number of grains, S_i denotes the Voronoï sites and r_i the corresponding weight if Laguerre-Voronoi tessellation is considered.

$$\begin{cases} \alpha_{ij}(x) = \frac{1}{2} \left\| \overrightarrow{S_i S_j} \right\| - \frac{\overrightarrow{S_i S_j} \cdot \overrightarrow{S_i x}}{\left\| \overrightarrow{S_i S_j} \right\|^2}, & 1 \leq i, j \leq N_G, j \neq i, \\ \psi_i(x, 0) = \min_{j \in \llbracket 1, N_G \rrbracket, j \neq i} (\alpha_{ij}(x)), & 1 \leq i \leq N_G. \end{cases} \quad (2)$$

$$\begin{cases} \alpha_{ij}(x) = \frac{1}{2} \left(\left\| \overrightarrow{S_i S_j} \right\| + \frac{r_i^2 - r_j^2}{\left\| \overrightarrow{S_i S_j} \right\|^2} \right) - \frac{\overrightarrow{S_i S_j} \cdot \overrightarrow{S_i x}}{\left\| \overrightarrow{S_i S_j} \right\|^2}, & 1 \leq i, j \leq N_G, j \neq i \\ \psi_i(x, 0) = \min_{j \in \llbracket 1, N_G \rrbracket, j \neq i} (\alpha_{ij}(x)), & 1 \leq i \leq N_G. \end{cases} \quad (3)$$

This procedure presents the interest of being very simple to implement. However, its numerical cost is not negligible as it involves an N_G^2 algorithm at each integration point of the FE mesh. A numerical improvement (Hitti et al. 2012) consists in taking into account the dual of the Voronoï (resp. Laguerre-Voronoi) tessellation which corresponds to the Delauney (resp. weighted Delauney) triangulation which enables to limit the research of the minimum in Eqs. (2) and (3) to the *Graph* of each site in the obtained triangulation. Fig.3 illustrates, in LS context, polycrystals respecting an experimental grain size distribution thanks to a Laguerre-Voronoi tessellation.

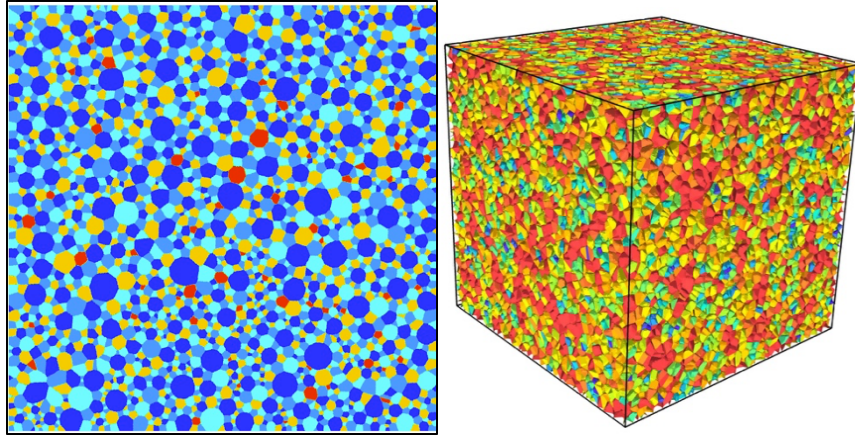


Figure 3. LS description in an unstructured FE mesh of a 304L polycrystal made of equiaxed grains generated thanks to a Laguerre-Voronoi tessellation: (left) 2D context with a polycrystal of 10000 grains described with 5 GLS and (right) 3D context with a polycrystal of 80.000 grains described with 17 GLS. The color code corresponds to the GLS identifier after applying the coloration technique described below.

Theoretically, each grain of a polycrystal must be represented by its own LS function. In order to reduce the computation time and memory storage, several non-neighboring grains in the initial microstructure (separated by a certain number of grains δ) can be grouped to form Global Level Set (GLS) functions thanks to *Graph* coloration technique. However, the grains belonging to the same function can no longer be distinguished. As a consequence, when two child grains of a GLS grow and meet each other, numerical coalescence occurs, i.e. both grains merge to form a single grain. Thus different strategies can be found in order to avoid or at least minimize numerical coalescence events: the initial separation δ can be chosen small enough to limit the computation time and sufficiently high to avoid a significant amount of coalescence (Cruz-Fabiano, Logé, and Bernacki 2014), a complete optimal coloration can be performed at each time step, or re-coloration algorithms can be considered at each time step (Krill III and Chen 2002; Elsey, Esedoğlu, and Smereka 2009; Scholtes et al. 2015).

Meshing adaptatation

In context of polyhedral cells, FE meshing of digital microstructures is quite straightforward, and consists, classically, in discretizing cells facets, and then the volume within each cell (Quey, Dawson, and Barbe 2011). This procedure is commonly used if the simulation domain is subjected to small deformations. Moreover, for real polycrystals, observed using Scanning Electron Microscopy (SEM) or 3D X-ray imaging techniques (Ludwig et al. 2009; Proudhon et al. 2016), a Voronoï/Laguerre-Voronoï mesh is not accessible. While there has been much research done on meshing methods for real 3D microstructures (Young et al. 2008; Y. Zhang, Bajaj, and Sohn 2005), the generalization of these methods to massively multiphase materials such as polycrystals is not straightforward (Rollett et al. 2004; Brahme et al. 2006). The main challenge is linked to multiple junctions, namely interfaces between more than two grains where respecting experimental data and achieving high mesh element quality can be complex.

Once a mesh has been generated as explained above, modeling large plastic strains and subsequent microstructure evolutions in FE framework is also very challenging. As a consequence, many researchers have chosen to avoid the use of conform meshes (i.e. where grain boundaries are explicitly meshed), and instead use implicit interface methods such as LS and MPF. While results using explicit interface methods are either restricted to limited deformations or based on a full reconstruction of the computational mesh at each time step (Hallberg 2013), implicit interface methods allow modeling of a wider range of metallurgical phenomena where large deformations are considered (Bernacki et al. 2009;

Scholtes et al. 2015; Scholtes, Boulais-Sinou, et al. 2016; Maire et al. 2017). However, this numerical strategy generally requires fine FE meshes at the grain interfaces to reach acceptable accuracy with regards to ReX and GG modeling. The absence of a conform mesh at grain boundaries generally requires a finer discretization. Of course, global isotropic refinement of the mesh or high order interpolation of LS functions can be used to reach a desired accuracy in the interface description, however, these strategies lead to a significant increase of computation resources. Adaptive local isotropic or anisotropic remeshing is therefore generally preferred. Different ways exist to generate locally adapted meshes to zero-isovalue of LS but, classically, metric field and topological meshers based on local mesh topology optimizations are used (Gruau and Coupez 2005; Coupez, Digonnet, and Ducloux 2000; Shakoor, Bernacki, and Bouchard 2015). Concerning metric calculations, the most common approach consists in using a posteriori error analysis in order to obtain an optimal mesh for a given number of nodes (Almeida et al. 2000; Coupez 2011). However, this approach can be non-optimal in polycrystal cases when an important number of LS functions must be considered. When describing strictly disjoint objects by LS functions, a simple solution consists in adapting the mesh thanks to a posteriori error estimator to $\phi(x, t) = \max_i(\psi_i(x, t))$. However, such an approach, used in (Scholtes et al. 2015; Maire et al. 2016), is not straightforward when the different objects considered are not strictly disjoint, which is the case in polycrystalline microstructures, as the ϕ function is then not derivable at the grain boundary network.

Alternatively, automatic geometrical methods can be used for the generation of local refined isotropic or anisotropic meshes adapted to polycrystals, based on the normal and/or mean curvature of the grain interfaces (Hitti et al. 2012; Bernacki et al. 2009). Fig. 4 illustrates a 2D exemple where anisotropic metric is considered thanks to a geometric approach (Bernacki et al. 2009) for an Inconel® 718 microstructure: the mesh is adapted to the grain interfaces (generated statistically with a Laguerre-Voronoi approach) and to second phase particles (SPP) interfaces immersed after thresholding of a SEM image. Fig 5 illustrates a 3D 304L case where a posteriori metric is adopted (Scholtes et al. 2015).

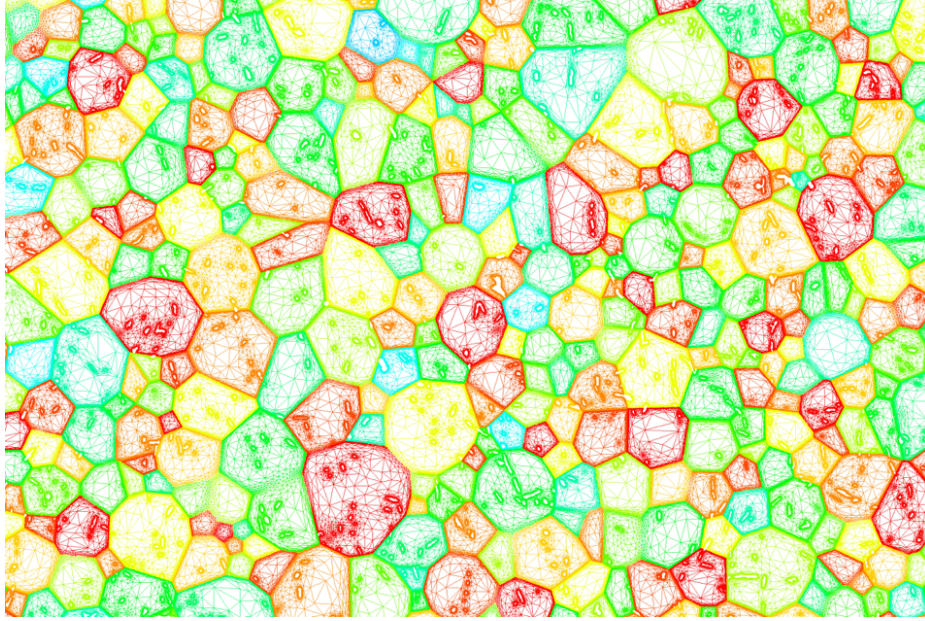


Figure 4. 2D Inconel@ 718 microstructure exemple where local anisotropic metric is considered for the FE mesh generation thanks to a geometric approach (Bernacki et al. 2009). The mesh is adapted to the grain interfaces (generated statistically with a Laguerre-Voronoi approach) and to delta phase interfaces immersed thanks to a SEM image. The color code corresponds to the GLS functions.

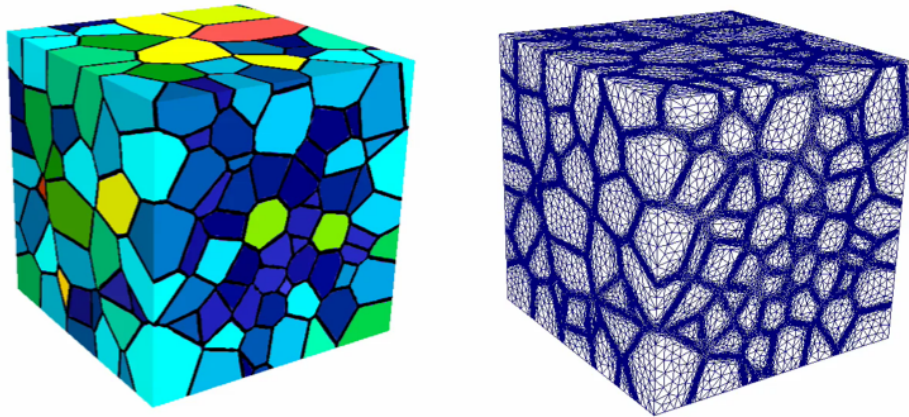


Figure 5. 3D equiaxed microstructure exemple where where local anisotropic metric is considered for the FE mesh generation thanks to a posteriori approach (Scholtes et al. 2015). The mesh is adapted to the grain interfaces (generated statistically with a Voronoi tessellation).

Interestingly, recent results have shown that the use of local meshing refinement could be questionable in 3D concerning the reduction of numerical cost comparatively to the use of static fine mesh (Scholtes 2016). Indeed, the numerical cost of frequent remeshing operations in 3D can also be very expensive. New strategies, maintaining the benefits of the classical Eulerian LS framework, while enforcing the conformity of the FE mesh to implicit interfaces in order to limit the use of very fine mesh at grain interfaces appears as an interesting alternative for 3D calculations (Florez et al. 2019).

Classical isotropic framework for LS modeling of ReX and GG

In the LS method, the evolution of $\psi(x, t)$ is given by the following transport equation (Osher and Sethian 1988):

$$\begin{cases} \frac{\partial \psi_i(x, t)}{\partial t} + \vec{v}(x, t) \cdot \nabla \psi_i(x, t) = 0 \\ \psi_i(x, t = 0) = \psi_i^0(x) \end{cases}, \quad \forall i \in \llbracket 1, N_{GLS} \rrbracket. \quad (4)$$

where $\vec{v}(x, t)$ is the velocity field and N_{GLS} the number of GLS functions. It is generally assumed for metals that the kinetics of grain boundary migration at the mesoscopic scale can be described as (F. J. Humphreys and Hatherly 2004):

$$\vec{v} = MP\vec{n}, \quad (5)$$

where M is the grain boundary mobility, P is the net driving pressure i.e. the net driving force per unit area, and \vec{n} is the outward unit normal to the GB. In context of deterministic full field approaches and neglecting torque terms (Fausty et al. 2018), the net pressure is classically defined as:

$$P = \tau \llbracket \rho \rrbracket - \gamma \kappa, \quad (6)$$

where τ is the dislocation line energy, $\llbracket \rho \rrbracket$ is the dislocation density jump across the interface, γ is the GB energy and κ is the mean GB curvature (i.e. the curvature in 2D and the sum of main curvatures in 3D). That is the GB motion is governed by the stored energy gradient across the GBs and by capillarity. The isotropy hypothesis remains here to consider M as being only dependant on temperature and γ as being constant. Assuming that $\|\nabla \psi_i(x, t)\| = 1, \forall i \in \llbracket 1, N_{GLS} \rrbracket$, i.e. ψ_i remain distance functions all along the simulation, after substituting Eq.(6) into Eq.(5) and

Eq.(5) into Eq.(4), and by considering the following properties of distance functions with the chosen sign convention:

$$\vec{n}_i = -\frac{\nabla\psi_i}{\|\nabla\psi_i\|} = -\nabla\psi_i, \quad \kappa_i = \nabla \cdot \vec{n}_i = -\Delta\psi_i, \quad (7)$$

one can solve a set of N_{GLS} convective-diffusive equations to take into account Eq.(5) for all the grains of the considered polycrystal (Bernacki, Logé, and Coupez 2011):

$$\begin{cases} \frac{\partial\psi_i(x,t)}{\partial t} - M\gamma\Delta\psi_i(x,t) + \vec{v}_i^{\llbracket\rho\rrbracket} \cdot \nabla\psi_i(x,t) = 0 \\ \psi_i(x,t=0) = \psi_i^0(x) \\ \vec{v}_i^{\llbracket\rho\rrbracket} = M\tau\llbracket\rho\rrbracket_i\vec{n}_i \end{cases}, \quad \forall i \in \llbracket 1, N_{GLS} \rrbracket. \quad (8)$$

Generally, a particular numerical treatment must be imposed to avoid kinematic incompatibilities after the resolution of Eq.(8). Indeed, voids can appear at multiple junctions and must be treated. A classical solution consists in correcting the GLS functions as follows (Merriman, Bence, and Osher 1994):

$$\tilde{\psi}_i(t,x) = \frac{1}{2} \left(\psi_i(t,x) - \max_{k \neq i}(\psi_k(t,x)) \right), \quad \forall i \in \llbracket 1, N_{GLS} \rrbracket. \quad (9)$$

The effect of Eq. (9) is schematized in Fig. 6. An alternative could also consist (Zhao et al. 1996) in closing void regions thanks to an energy minimization principle enforced by a Lagrange multiplier related to a constraint added to Eq.(4).

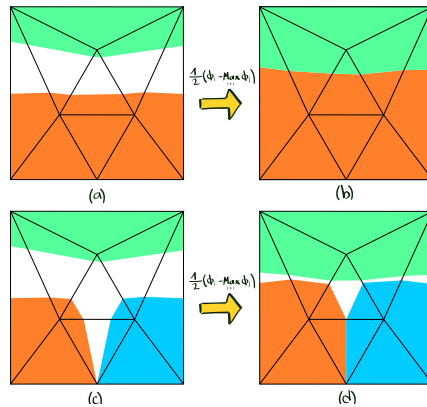


Figure 6. Global treatment to eliminate non-physical vacuum regions on a FE discretization: two colored LS (a) with a vacuum region in between them, (b) result after applying Eq. (9). Three colored LS : (c) with a vacuum region (d) result after applying Eq. (9).

A major drawback of the LS formulation lies in the fact that after the resolution of Eqs. (8) and (9), the GLS are no longer distance functions $\|\nabla\psi_i\| \neq 1$. This is particularly problematic when a specific remeshing technique depending on the distance property is used at the interface as described in the previous section. In addition, the convective-diffusive formulation proposed in Eq.(8) requires a distance function at least in a thin layer around the interface in order to compute properly the curvature driven mechanism. Finally, the conditioning of the transport problem also depends on the regularity of the LS function (Bernacki et al. 2009). For these reasons, the GLS functions need to be reinitialized. Restoring the metric property at the instant t is equivalent to solving the following eikonal equation:

$$\begin{cases} \|\nabla\psi_i(x, t)\| = 1, x \in \Omega \\ \psi_i(x, t) = 0, x \in \Gamma_i(t) \end{cases} \quad \forall i \in \llbracket 1, N_{GLS} \rrbracket. \quad (10)$$

Different approaches exist to solve this equation including the well-known Fast Marching Method introduced by Sethian (J. A. Sethian 1996) which propagates a front from the interface and ensures directly a gradient equal to unity. Though this approach has been extended to unstructured meshes (Kimmel and Sethian 1998), its implementation becomes complicated when it comes to consider anisotropic triangulations (James A Sethian and Vladimirsky 2003) and parallel efficiency is poor.

In (Sussman, Smereka, and Osher 1994), a Hamilton–Jacobi (H–J) formulation equivalent to Eq.(10) was proposed in order to correct iteratively the level set values around the interface by solving a partial differential equation (PDE). This method is massively used in the LS modeling of ReX and GG (Agnoli et al. 2014; Cruz-Fabiano, Logé, and Bernacki 2014; Bernacki, Logé, and Coupez 2011; Hallberg and Bulatov 2019). It requires the definition of a purely numerical parameter known as a fictitious time step for reinitialization and the ratio between the desired reinitialized thickness and this parameter gives the number of required increments. Coupled convection-reinitialization (CR) methods emerged wherein the LS function is automatically reinitialized during the resolution of the transport equation (Coupez 2007; Bernacki et al. 2008, 2009). Their main advantage lies in the fact that only one solver is needed for the simulation instead of two for the classical H–J technique. The signed distance function can also be replaced by any smooth function which satisfies the metric property, at least in a thin layer around the interface.

Finally, a natural way to reinitialize GLS functions consists in using a brute force algorithm to perform a complete reconstruction of the distance function. This technique works in two steps: discretize the interface (zero-iso-value of the LS function) into a collection of simple elements and, for every node, compute the distance to all elements of the collection and store the smallest value which becomes the updated value of the distance function. Though it guarantees optimal accuracy, this

Direct Reinitialization (DR) technique is generally reported as being greedy in terms of computational requirements (Sussman, Smereka, and Osher 1994; Elias, Martins, and Coutinho 2007; Jones, Baerentzen, and Sramek 2006). It is nevertheless worth mentioning that these works generally address only regular grids or hierarchical meshes (Fortmeier and Martin Bucker 2011). Recently, a new direct fast and accurate approach usable in unstructured FE mesh has been proposed (Shakoor et al. 2015). This method takes advantage of a space-partitioning technique using k - d tree and an efficient bounding box strategy enabling to maximize the numerical efficiency for parallel computations. Discussions concerning the residual errors inherent to this approach is also discussed in (Florez and Bernacki 2019).

By extrapolating the shape of the velocity term, $\vec{v}_i^{[\rho]}$ of Eq.(8), for the interface between grain G_i and G_j , the corresponding velocity $\vec{v}_{ij}^{[\rho]}$ can be written as:

$$\vec{v}_{ij}^{[\rho]} = M\tau_{ij}^{[\rho]}\vec{n}_{ij}. \quad (11)$$

Classically in LS or MPF approaches, a constant stored energy is considered in each grain (Bernacki et al. 2008, 2009; Logé et al. 2008; Resk et al. 2009; Scholtes, Boulais-Sinou, et al. 2016; Hallberg 2013; Elsey, Esedoğlu, and Smereka 2009; Maire et al. 2017). Then, for each interface between grain G_i and G_j , it is assumed that:

$$\tau_{ij}^{[\rho]} = e_j - e_i, \quad (12)$$

where e_i and e_j are the mean stored energies in the grains G_i and G_j , respectively.

These averages can directly come from either constant approximative values where only a gradient of the stored dislocations between the nuclei and the non-recrystallized grains is considered as in (Bernacki et al. 2008; Bernacki, Logé, and Coupez 2011; Elsey, Esedoğlu, and Smereka 2009), or simplified mechanical formulations as in (Maire et al. 2017). They can also be evaluated thanks to an existing dislocation field in the FE mesh of the calculation domain Ω as in (Maire et al. 2016; Bernacki et al. 2009; Logé et al. 2008; Hallberg 2013; Scholtes, Boulais-Sinou, et al. 2016) or come from a dislocation density field measured from experimental data, immersed in the FE mesh and averaged per grain as in (Agnoli et al. 2015; Villaret et al. 2019).

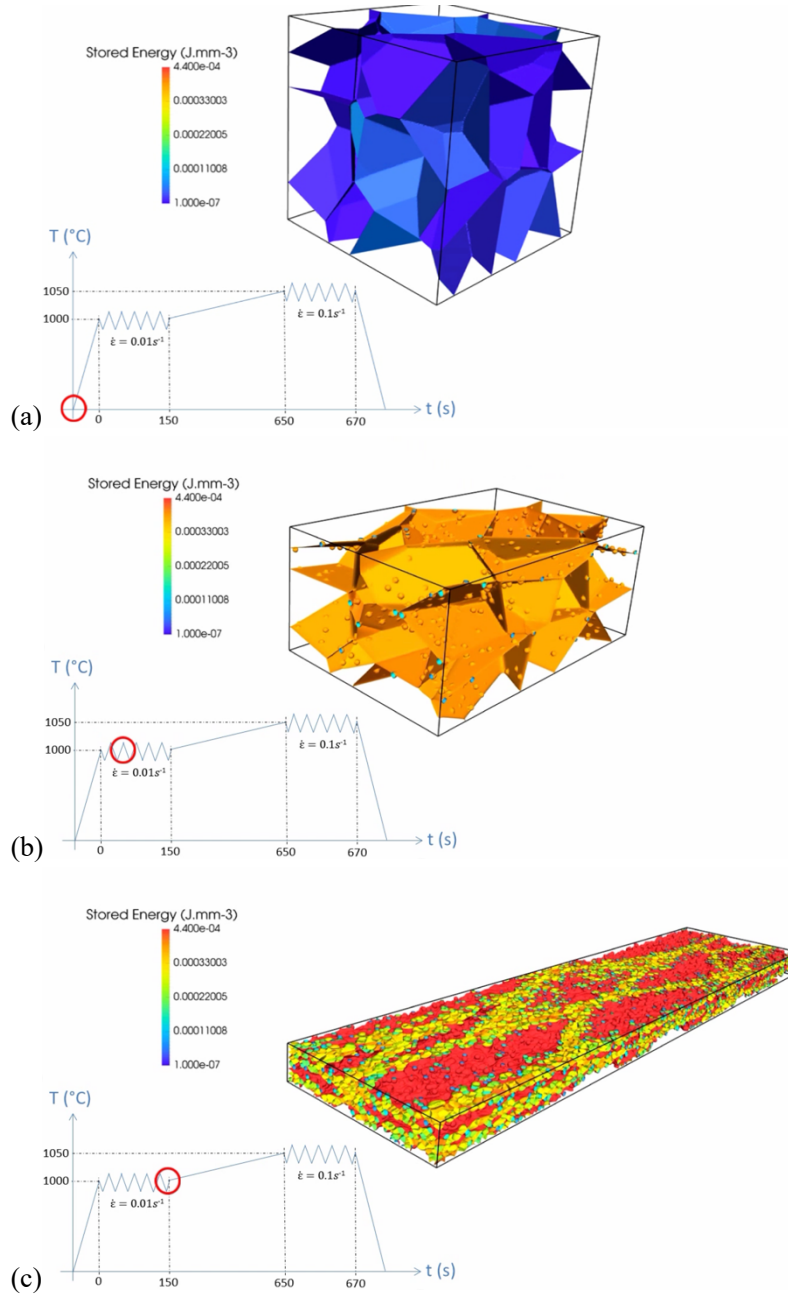
Special attention has to be paid to the velocity field $\vec{v}^{[\rho]}$ in the vicinity of multiple junctions as emphasized in (Bernacki et al. 2008). In fact, rather than

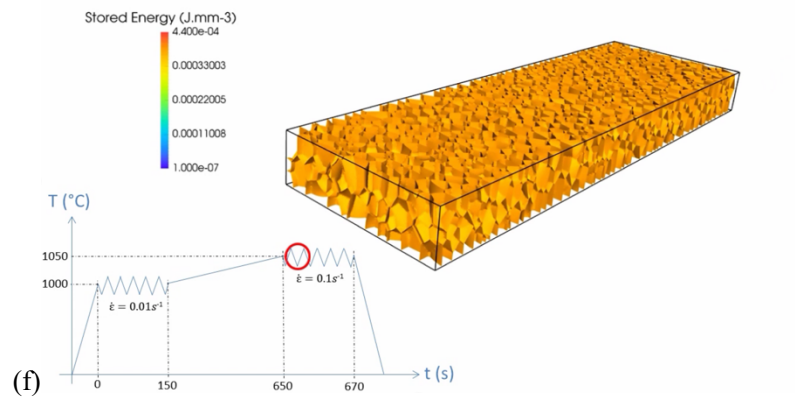
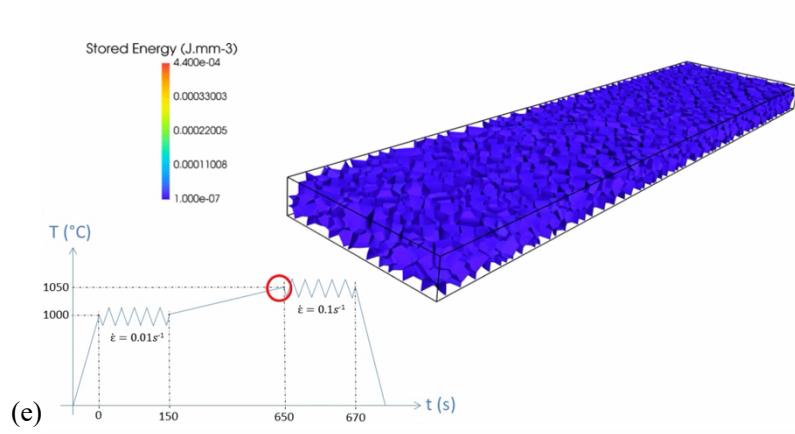
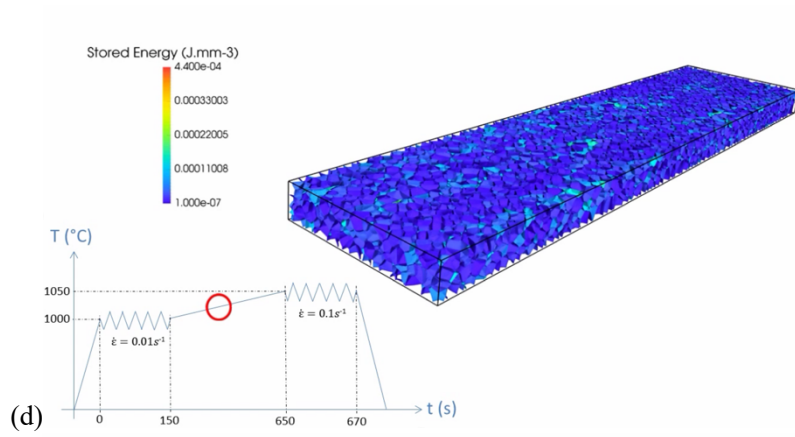
dealing with $\vec{v}_i^{[\rho]}$ per grain as described in Eq.(8) and considering the contributions of each neighbor as in Eq.(11), a global common velocity can be built in the calculation domain and used for each convection-diffusion system. 3D results obtained this way are summarized in Fig. 7 for a complex thermomechanical path applied onto 304L stainless steel. The microstructure is initially generated by a Laguerre-Voronoi strategy as detailed in (Hitti et al. 2012). The system of equations (8) is solved by considering Eqs (9), (11), (12), an optimized graph recoloration technique (Scholtes et al. 2015), a direct reinitialization technique (Shakoor et al. 2015) and the simplified mechanical framework detailed in (Maire et al. 2017).

Anisotropy of grain interface energy

GG thermodynamics are relatively complex due to the “macroscopic” dimensionality of the grain boundaries (Sutton and Balluffi 1995). When dealing with heterogeneous phenomena (thermal twinning, plastic localization, onset of fracture, etc.), material heterogeneities must be taken into account. As such, calculations used to predict microstructure after thermomechanical processing must be improved and enriched to take into account local properties such as non-uniform or anisotropic grain interface energy. The five-dimensional space of grain boundaries is non-Euclidean and partitioned into symmetric subspaces due to the inherent crystallography of the material. The topology of the grain boundary space makes it difficult to define a metric (Morawiec 2009; Olmsted 2009) which makes any multivariate calculus one wishes to perform, such as that required by the finite element method (FEM). It must be highlighted that if GG studies with non-uniform grain boundary energy are numerous (Yu, Nosonovsky, and Esche 2009; Grest, Srolovitz, and Anderson 1985; Sieradzki and Madej 2013), the difficulties concerning a clear description of the grain boundary energy and accounting for its successive derivatives which have an impact of the capillarity driving pressure remains an unsolved issue in the state of the art.

Several anisotropic full field grain growth frameworks also exist based on LS and MPF approaches (Miyoshi and Takaki 2017; Chang et al. 2017; Chang and Moelans 2014; Mallick and Vedantam 2009; Jin et al. 2015; Hallberg 2014; Hallberg and Bulatov 2019; Elsey, Esedođlu, and Smereka 2013; Fausty et al. 2018; Fausty, Bozzolo, and Bernacki 2019). Of particular note is the relatively new MPF formulation used in (Miyoshi and Takaki 2017), which allows for both the definition of heterogeneous grain boundary energies and mobilities, and the MPF method applied in (Chang et al. 2017), which shows very interesting results in special dual grain boundary microstructures. However, both formulations suffer from inherent numerical instabilities when increasing the heterogeneity of the system. Concerning the LS method, (Elsey, Esedođlu, and Smereka 2013) define a grain boundary energy “per grain” and then use an adhoc averaging





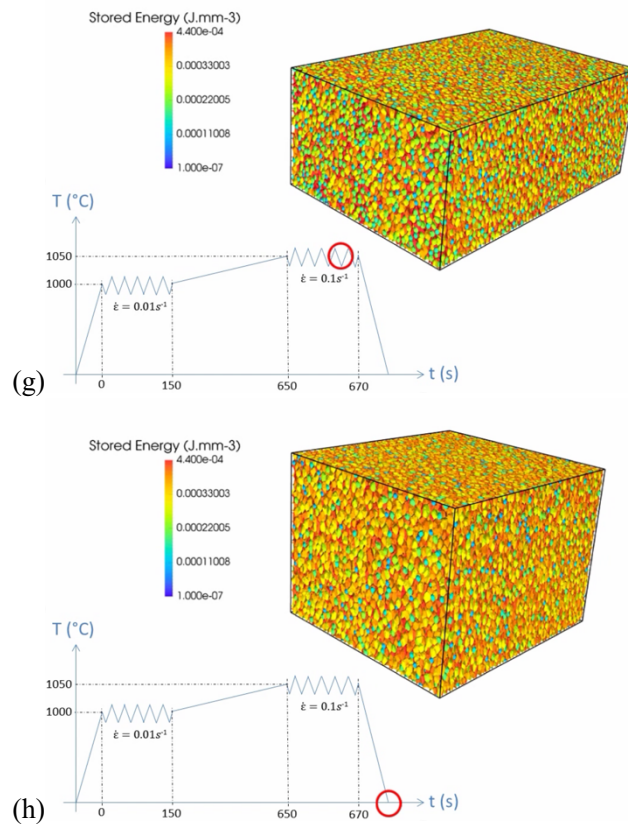


Figure 7. Complex thermomechanical path for a 304L stainless steel. In each picture from (a) to (h), the red circle describes the corresponding position in the thermomechanical path (t (s) in abscissa and T (°C) in ordinate, zigzag lines symbolize deformation steps, straight lines symbolize annealing steps) and the microstructure predicted at the same time with the grain boundary network colored by the stored energy. (a) corresponds to the initial state, (b) corresponds to the beginning of DRX with appearance of few nuclei at the existing grain interfaces, the deformation ($\dot{\epsilon} = 0.01 \text{ s}^{-1}$) is applied along the z-direction, (c) corresponds to the end of the first deformation; (d) and (e) described the post-deformation evolution during an increase of temperature, MDRX, SRX and GG mechanisms occur; (f) and (g) describe a second deformation ($\dot{\epsilon} = 0.1 \text{ s}^{-1}$) along the x-direction with a second DRX evolution and finally (h) described the final state obtained after quenching.

operation to define the energy at the interface between two grains. They then solve the grain growth problem isotropically using the highest grain boundary energy

followed by a mathematical procedure to correct the evolution of the grain boundary network to take into account the presence of multiple boundary energies.

This approach was also studied and validated in (Jin et al. 2015). However, this framework is almost exclusively geometric and, at the triple junctions, the authors define a seemingly arbitrary junction energy in order to obtain the correct behavior of the system. The authors in (Hallberg 2014) use another method which imposes isogonic point triple junctions and solves curvature driven grain growth for heterogeneous grain boundary energies. Other very recent work (Hallberg and Bulatov 2019) goes so far as to simulate on regular grids the full anisotropic case (misorientation and inclination dependent grain boundary energy) using a LS formulation close to the one proposed in (Fausty et al. 2018) in FE context. In (Fausty, Bozzolo, and Bernacki 2019), the formulation proposed in (Fausty et al. 2018) is applied to single phase 2D polycrystals to explore the sensitivity of this numerical framework to variations in its numerical parameters as well as the effect that different grain boundary energy functions can have on the development of a material microstructure.

In conclusion, a reasonable questioning can still emerge from all the cited literature concerning the dependence of the grain boundary energy to the inclination of the boundary as well as the misorientation rotation axis. For example, the impact of the torque terms generated by inclination dependent grain boundary energies are systematically neglected. They cannot be simply expressed by the contraction of gradient of the grain boundary energy function on the normal given the tangentiality of this gradient field to the grain boundary surface far away from boundary junctions. As such, supplemental terms depending on both γ and the boundary geometry should probably be developed and integrated in the coming years in the existing full field formulations to aspire to a fully anisotropic formulation for grain growth.

Static second phase particles

As described by the well-known Smith-Zener model (Smith 1948; F. J. Humphreys and Hatherly 2004), precipitates act as obstacles to the displacement of the grain boundaries and may hinder grain growth. Under certain conditions, Second Phase Particles (SPP) can pin the microstructure, leading eventually to a limiting mean grain size (MGS), which is characteristic of the Smith-Zener pinning. This phenomenon is widely used by metallurgists to control the grain size during the forming process of many alloys, including superalloys. Predictive tools are then needed to model accurately this phenomenon and thus optimize the final grain size

and in-use properties of the materials. Classical laws predicting the limiting MGS (Manohar, Ferry, and Chandra 1998), noted \bar{R}_∞ , have the following form:

$$\bar{R}_\infty = K \frac{\bar{r}}{f^m}, \quad (13)$$

where r and f describe, the mean radius and volume (surface in 2D) fraction of SPP, respectively. K and m are two parameters that fluctuate according to the assumptions made to obtain the equation (Manohar, Ferry, and Chandra 1998; Agnoli et al. 2014). Since thirty years, numerous full field modeling of the Smith-Zener phenomenon have been proposed, including MC/CA framework (Srolovitz et al. 1984; Anderson et al. 1989; Hassold, Holm, and Srolovitz 1990; Gao, Thompson, and Patterson 1997; Kad and Hazzledine 1997; Phaneesh et al. 2012), front tracking or vertex (Weygand, Brechet, and Lépinoux 2001; Couturier, Maurice, and Fortunier 2003), MPF (Chang, Feng, and Chen 2009; Tonks et al. 2015; Moelans, Blanpain, and Wollants 2006; Chang and Moelans 2015) and LS (Agnoli et al. 2012, 2015, 2014; Scholtes et al. 2015; Villaret et al. 2019).

Concerning the LS framework, the idea to consider inert SPP in a FE framework has been first proposed to perform 2D GG (Agnoli et al. 2012) and 2D static recrystallization (Agnoli et al. 2014) simulations for Inconel® 718. SPP are inserted in the FE mesh thanks to statistical description or experimental data and the local curvature of the grain boundaries in contact with SPP is constrained. This approach enables to consider SPP with no assumption on their size or morphology, isotropic and anisotropic particle/grain interface energies (incoherent or coherent interfaces) can be simply considered by applying the appropriate boundary conditions. The dragging effect is naturally modeled by the modification of the local curvature when the grain boundary encounters the particles, which implies that no assumption is made on the dragging force exerted by the particles. This approach was used to support the idea that the phenomenon reported as abnormal grain growth in Inconel® 718 could be explained by the growth of lower energy grains in a pinned microstructure and as such be a particular case of static recrystallization. Thanks to these simulations, the sensitivity of this phenomenon to the initial stored energy distribution could be studied (Agnoli et al. 2015). Optimization of parameters K and m of Eq.(13) thanks to a full field simulations campaign and first 3D LS simulations were proposed in (Scholtes, Ilin, et al. 2016) and (Scholtes et al. 2015), respectively. Recently comparisons with MC simulations and experimental data have been made for ODS steels (Villaret et al. 2019). Figure 8

illustrates a 3D GG LS simulations for Inconel® 718 with an idealized spherical population of SPP ($f = 3\%$), until reaching a final stable microstructure.

Industrial applications

As emphasized in the introduction, full field modeling of ReX and GG in context of industrial thermomechanical conditions is rare in the state of the art and first cases were proposed recently thanks to a LS-FE framework available in the DIGIMU® software package. The following describes briefly the global microstructure simulation approach used in this software allowing a multiscale modeling of ReX phenomenon from material identification to industrial-like process simulations.

A precise knowledge of the thermomechanical history of the process is required to make relevant microstructural predictions at given integration points. Macroscopic simulations must be performed with a specific attention given to mechanical and thermal boundary conditions, as well as friction modelling. As the velocity gradient is a particularly unstable value in simulations, mesh must be fine enough to obtain smooth evolutions at the position of interest concerning the mesoscopic simulations. In case of high temperature gradients at the macroscale boundaries, adapting the mesh is essential to describe accurately the temperature field evolution. Some typical calculations in this context are described in (Micheli, Maire, Moussa, et al. 2019) for a 2D cogging and a 3D close die forging simulations and in (Micheli, Maire, Cardinaux, et al. 2019) for a 2D hot plate rolling process. Once the temperature and strain rate fields are known from the macroscopic simulation, material characterization can begin.

A material parameter identification procedure (reduced mobility, hardening, recovery and ReX parameters) based on experimental tests, mean field and full field calibration simulations is proposed in the DIGIMU® software package. Indeed, material parameter identification is unavoidable to obtain accurate microstructural predictions, whatever the type or the complexity of the used model. The question is how much experiments must be performed to obtain a broad enough description of the material. The identification of a set of parameters for a non physical model will require as many experiments as for a physical model, but the range of validity of the physical model will be much better than the range of validity

of the non physical one. Details on such identification procedure can be found in (Maire et al. 2019; Micheli, Maire, Moussa, et al. 2019).

Conclusions and perspectives

In the last decades, full field approaches have been extensively developed to simulate microstructure evolution during forming processes. Modeling at the mesoscopic scale can give insight into the understanding of complex microstructural phenomena but it can also be used to optimize/calibrate higher scale models (like mean field models or phenomenological ones). These simulations allow describing the material microstructure features in a natural way. The recent improvements done to reduce the high computation times typical of such models make possible nowadays their use for industrial applications. Within this context, the development of numerical models able to predict microstructure evolution, at the mesoscopic scale is of prime importance. These digital models will allow being very reactive to new markets with confidence in the proposed manufacturing routes and parameters.

Furthermore, scientific perspectives in terms of understanding and modeling of metallurgical phenomena and development of the LS methodology are then as ambitious as the industrial perspectives in terms of applications. As current improvement of this approach, one can cite works dedicated to i) reducing the numerical cost (Florez et al. 2019), ii) the enrichment of the driving pressure description by considering richer physical description of the grain boundary energy (Fausty, Bozzolo, and Bernacki 2019; Hallberg and Bulatov 2019) and of the grain boundary mobility (Murgas et al. 2019), iii) the modeling of other mechanisms leading to interfaces boundary motion such as spherodization of lamellar microstructures (Polychronopoulou et al. 2017) or more globally diffusive solid/solid phase transformation (Bernacki et al. 2019; Alvarado et al. 2019).

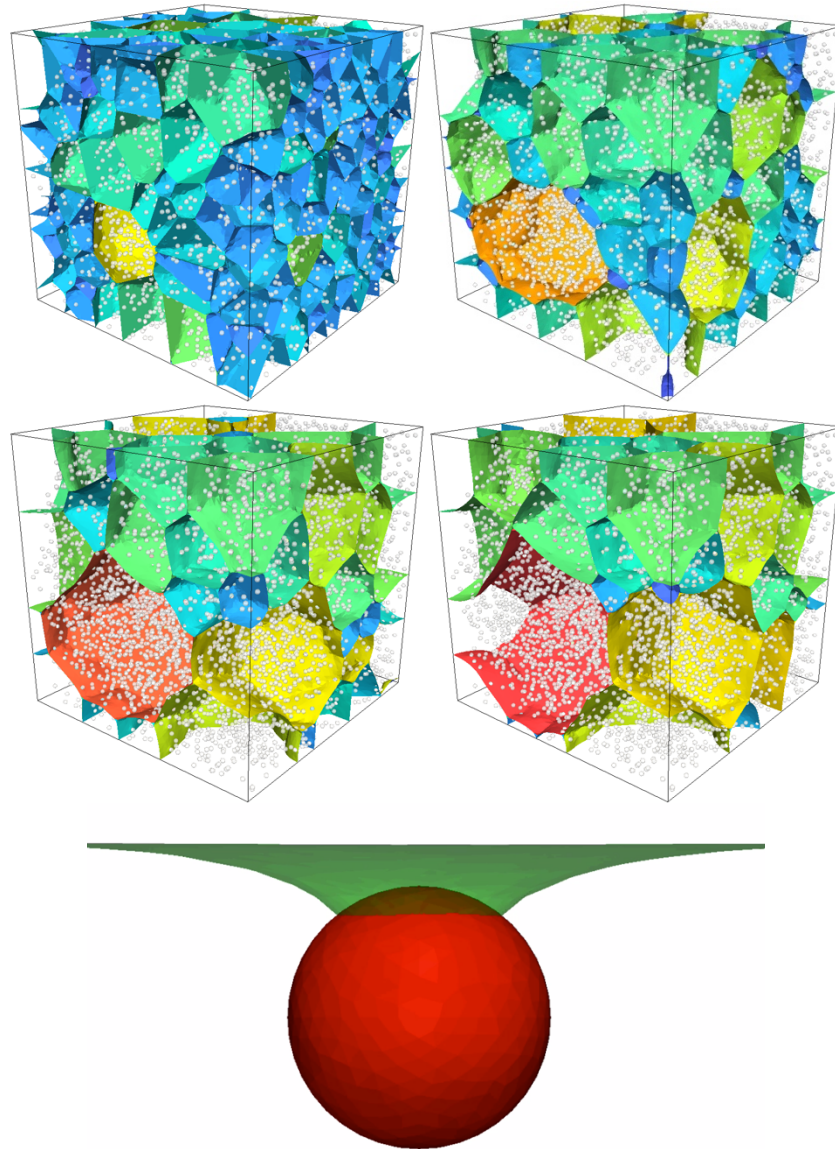


Figure 8. 3D GG LS simulations for Inconel@ 718 with an idealized spherical population of second phase particles ($f=3\%$). SPP are described in white, the grain boundary network is described with a color code corresponding to the grain size until a stable configuration. From top to bottom and left to right: time evolution during the thermal treatment from the initial configuration to the stable grain boundary network. The last image corresponds to a zoom of a SPP (in red) interacting with one GB (in green).

REFERENCES

- Agnoli, A., M. Bernacki, R. Logé, J.-M. Franchet, J. Laigo, and N. Bozzolo. 2012. "Understanding and Modeling of Grain Boundary Pinning in Inconel 718." In *Superalloys 2012*. <https://doi.org/10.1002/9781118516430.ch8>.
- . 2015. "Selective Growth of Low Stored Energy Grains During δ Sub-Solvus Annealing in the Inconel 718 Nickel-Based Superalloy." *Metallurgical and Materials Transactions A*. <https://doi.org/10.1007/s11661-015-3035-9>.
- Agnoli, A., N. Bozzolo, R. Logé, J.-M. Franchet, J. Laigo, and M. Bernacki. 2014. "Development of a Level Set Methodology to Simulate Grain Growth in the Presence of Real Secondary Phase Particles and Stored Energy – Application to a Nickel-Base Superalloy." *Computational Materials Science* 89 (June): 233–41. <https://doi.org/10.1016/j.commatsci.2014.03.054>.
- Almeida, R. C., R. A. Feijóo, A. C. Galeão, C. Padra, and R. S. Silva. 2000. "Adaptive Finite Element Computational Fluid Dynamics Using an Anisotropic Error Estimator." *Computer Methods in Applied Mechanics and Engineering* 182 (3–4): 379–400. [https://doi.org/10.1016/S0045-7825\(99\)00200-5](https://doi.org/10.1016/S0045-7825(99)00200-5).
- Alvarado, K., B. Flipon, J. Blaizot, N. Bozzolo, and M. Bernacki. 2019. "Influence of Zener Pinning Phenomena on the Size Homogeneity of Recrystallized Grains: Multiscale Approach and Application to Nickel-Base Superalloys." In *Colloque "La Métallurgie, Quel Avenir!"*
- Anderson, M. P., G. S. Grest, R. D. Doherty, K. Li, and D. J. Srolovitz. 1989. "Inhibition of Grain Growth by Second Phase Particles: Three Dimensional Monte Carlo Computer Simulations." *Scripta Metallurgica* 23 (5): 753–58. [https://doi.org/10.1016/0036-9748\(89\)90525-5](https://doi.org/10.1016/0036-9748(89)90525-5).
- Avrami, M. 1939. "Kinetics of Phase Change, I. General Theory." *Journal of Chemical Physics* 7: 1103–12.
- Bagi, K. 1993. "A Quasi-Static Numerical Model for Micro-Level Analysis of Granular Assemblies." *Mechanics of Materials* 16 (1–2): 101–10. [https://doi.org/10.1016/0167-6636\(93\)90032-M](https://doi.org/10.1016/0167-6636(93)90032-M).
- . 2005. "An Algorithm to Generate Random Dense Arrangements for Discrete Element Simulations of Granular Assemblies." *Granular Matter* 7 (1): 31–43. <https://doi.org/10.1007/s10035-004-0187-5>.
- Beltran, O., K. Huang, and R. E. Logé. 2015. "A Mean Field Model of Dynamic and Post-Dynamic Recrystallization Predicting Kinetics, Grain Size and Flow Stress." *Computational Materials Science*. <https://doi.org/10.1016/j.commatsci.2015.02.043>.
- Benabbou, A., H. Borouchaki, P. Laug, and J. Lu. 2009. "Geometrical Modeling of Granular Structures in Two and Three Dimensions. Application to Nanostructures." *International Journal for Numerical Methods in Engineering* 80 (4): 425–54. <https://doi.org/10.1002/nme.2644>.
- Bernacki, M., Y. Chastel, T. Coupez, and R.E. Logé. 2008. "Level Set Framework for the Numerical Modelling of Primary Recrystallization in Polycrystalline Materials." *Scripta Materialia* 58 (12): 1129–32.

- <https://doi.org/10.1016/j.scriptamat.2008.02.016>.
- Bernacki, M., H. Dignonnet, H. Resk, T. Coupez, and R. Logé. 2007. "Development of Numerical Tools for the Multiscale Modelling of Recrystallization in Metals, Based on a Digital Material Framework." In *AIP Conference Proceedings*. Vol. 908. <https://doi.org/10.1063/1.2740840>.
- Bernacki, M., R.E. Logé, and T. Coupez. 2011. "Level Set Framework for the Finite-Element Modelling of Recrystallization and Grain Growth in Polycrystalline Materials." *Scripta Materialia* 64 (6): 525–28. <https://doi.org/10.1016/j.scriptamat.2010.11.032>.
- Bernacki, M., C. T. Pham, N. Bozzolo, and C. Moussa. 2019. "A New Full Field Framework to Model Grain and Phase Boundaries Migration during Diffusive Solid/Solid Phase Transformations and Recrystallization." In *ReX & GG 2019 Proceedings*.
- Bernacki, M., H. Resk, T. Coupez, and R. E. Logé. 2009. "Finite Element Model of Primary Recrystallization in Polycrystalline Aggregates Using a Level Set Framework." *Modelling and Simulation in Materials Science and Engineering* 17 (6): 064006. <https://doi.org/10.1088/0965-0393/17/6/064006>.
- Bernard, P., S. Bag, K. Huang, and R.E. Logé. 2011. "A Two-Site Mean Field Model of Discontinuous Dynamic Recrystallization." *Materials Science and Engineering: A* 528 (24): 7357–67. <https://doi.org/10.1016/j.msea.2011.06.023>.
- Brahme, A., M.H. Alvi, D. Saylor, J. Fridy, and A.D. Rollett. 2006. "3D Reconstruction of Microstructure in a Commercial Purity Aluminum." *Scripta Materialia* 55 (1): 75–80. <https://doi.org/10.1016/J.SCRIPTAMAT.2006.02.017>.
- Chang, K., L.-Q. Chen, C. E. Krill, and N. Moelans. 2017. "Effect of Strong Nonuniformity in Grain Boundary Energy on 3-D Grain Growth Behavior: A Phase-Field Simulation Study." *Computational Materials Science* 127 (February): 67–77. <https://doi.org/10.1016/J.COMMATSCI.2016.10.027>.
- Chang, K., W. Feng, and L.-Q. Chen. 2009. "Effect of Second-Phase Particle Morphology on Grain Growth Kinetics." *Acta Materialia* 57 (17): 5229–36. <https://doi.org/10.1016/j.actamat.2009.07.025>.
- Chang, K., and N. Moelans. 2014. "Effect of Grain Boundary Energy Anisotropy on Highly Textured Grain Structures Studied by Phase-Field Simulations." *Acta Materialia* 64 (February): 443–54. <https://doi.org/10.1016/J.ACTAMAT.2013.10.058>.
- . 2015. "Phase-Field Simulations of the Interaction between a Grain Boundary and an Evolving Second-Phase Particle." *Philosophical Magazine Letters* 95 (4): 202–10. <https://doi.org/10.1080/09500839.2015.1031845>.
- Chen, L.-Q. 2002. "Phase-Field Models for Microstructure Evolution." *Annual Review of Materials Research* 32 (1): 113–40. <https://doi.org/10.1146/annurev.matsci.32.112001.132041>.
- Coupez, T. 2007. "Convection Of Local Level Set Function For Moving Surfaces And Interfaces In Forming Flow." In *AIP Conference Proceedings*, 908:61–66. AIP. <https://doi.org/10.1063/1.2740790>.
- . 2011. "Metric Construction by Length Distribution Tensor and Edge Based Error for Anisotropic Adaptive Meshing." *Journal of Computational Physics* 230

- (7): 2391–2405. <https://doi.org/10.1016/j.jcp.2010.11.041>.
- Coupez, T., H. Dignonnet, and R. Ducloux. 2000. “Parallel Meshing and Remeshing.” *Applied Mathematical Modelling* 25 (2): 153–75. [https://doi.org/10.1016/S0307-904X\(00\)00045-7](https://doi.org/10.1016/S0307-904X(00)00045-7).
- Couturier, G., C. Maurice, and R. Fortunier. 2003. “Three-Dimensional Finite-Element Simulation of Zener Pinning Dynamics.” *Philosophical Magazine* 83 (30): 3387–3405. <https://doi.org/10.1080/1478643031000152771>.
- Cram, D. G., H. S. Zurob, Y. J. M. Brechet, and C. R. Hutchinson. 2009. “Modelling Discontinuous Dynamic Recrystallization Using a Physically Based Model for Nucleation.” *Acta Materialia*. <https://doi.org/10.1016/j.actamat.2009.07.024>.
- Cruz-Fabiano, A.-L., R. Logé, and M. Bernacki. 2014. “Assessment of Simplified 2D Grain Growth Models from Numerical Experiments Based on a Level Set Framework.” *Computational Materials Science* 92 (September): 305–12. <https://doi.org/10.1016/j.commatsci.2014.05.060>.
- Cui, L., and C. O’Sullivan. 2003. “Analysis of a Triangulation Based Approach for Specimen Generation for Discrete Element Simulations.” *Granular Matter* 5 (3): 135–45. <https://doi.org/10.1007/s10035-003-0145-7>.
- Depriester, D., and R. Kubler. 2019. “Radical Voronoi Tessellation from Random Pack of Polydisperse Spheres: Prediction of the Cells’ Size Distribution.” *Computer-Aided Design* 107 (February): 37–49. <https://doi.org/10.1016/J.CAD.2018.09.001>.
- Elias, R. N., M. A. D. Martins, and Al. L. G. A. Coutinho. 2007. “Simple Finite Element-Based Computation of Distance Functions in Unstructured Grids.” *International Journal for Numerical Methods in Engineering* 72 (9): 1095–1110. <https://doi.org/10.1002/nme.2079>.
- Elsay, M., S. Esedoğlu, and P. Smereka. 2009. “Diffusion Generated Motion for Grain Growth in Two and Three Dimensions.” *Journal of Computational Physics* 228 (21): 8015–33. <https://doi.org/10.1016/j.jcp.2009.07.020>.
- . 2010. “Large-Scale Simulation of Normal Grain Growth via Diffusion-Generated Motion.” *Proceedings of the Royal Society A Mathematical Physical and Engineering Sciences* 467 (2126): 381–401. <https://doi.org/10.1098/rspa.2010.0194>.
- . 2013. “Simulations of Anisotropic Grain Growth: Efficient Algorithms and Misorientation Distributions.” *Acta Materialia* 61 (6): 2033–43. <https://doi.org/10.1016/J.ACTAMAT.2012.12.023>.
- Esedoğlu, S. 2016. “Grain Size Distribution under Simultaneous Grain Boundary Migration and Grain Rotation in Two Dimensions.” *Computational Materials Science*. <https://doi.org/10.1016/j.commatsci.2016.04.022>.
- Fausty, J., N. Bozzolo, and M. Bernacki. 2019. “A 2D Level-Set Finite Element Grain Coarsening Study with Heterogeneous Grain Boundary Energies.” *To Appear*.
- Fausty, J., N. Bozzolo, D. Pino Muñoz, and M. Bernacki. 2018. “A Novel Level-Set Finite Element Formulation for Grain Growth with Heterogeneous Grain Boundary Energies.” *Materials and Design* 160 (December): 578–90. <https://doi.org/10.1016/j.matdes.2018.09.050>.
- Florez, S., and M. Bernacki. 2019. “A New Fast and Robust Finite Element Strategy to

- Simulate Microstructural Evolutions.” *To Appear*.
- Florez, S., M. Shakoor, T. Toulorge, and M. Bernacki. 2019. “Body-Fitted Finite Element Discretizations for Moving Interfaces in Context of Microstructure Evolutions.” In *CSMA 2019 Proceedings*. <https://csma2019.sciencesconf.org/250729/document>.
- Fortmeier, Ol., and H. Martin Bucker. 2011. “Parallel Re-Initialization of Level Set Functions on Distributed Unstructured Tetrahedral Grids.” *Journal of Computational Physics* 230 (12): 4437–53. <https://doi.org/10.1016/J.JCP.2011.02.005>.
- Gao, J., R. G. Thompson, and B. R. Patterson. 1997. “Computer Simulation of Grain Growth with Second Phase Particle Pinning.” *Acta Materialia* 45 (9): 3653–58. [https://doi.org/10.1016/S1359-6454\(97\)00048-7](https://doi.org/10.1016/S1359-6454(97)00048-7).
- Garcke, H., B. Nestler, and B. Stoth. 1999. “A Multi Phase Field Concept: Numerical Simulations Of Moving Phase Boundaries And Multiple Junctions.” *SIAM J. Appl. Math.* 60: 295–315. <http://citeseerx.ist.psu.edu/viewdoc/summary?doi=10.1.1.8.1711>.
- Grest, G.S., D.J. Srolovitz, and M.P. Anderson. 1985. “Computer Simulation of Grain Growth—IV. Anisotropic Grain Boundary Energies.” *Acta Metallurgica* 33 (3): 509–20. [https://doi.org/10.1016/0001-6160\(85\)90093-8](https://doi.org/10.1016/0001-6160(85)90093-8).
- Gruau, C., and T. Coupez. 2005. “3D Tetrahedral, Unstructured and Anisotropic Mesh Generation with Adaptation to Natural and Multidomain Metric.” *Computer Methods in Applied Mechanics and Engineering* 194 (48–49): 4951–76. <https://doi.org/10.1016/j.cma.2004.11.020>.
- Hallberg, H. 2013. “A Modified Level Set Approach to 2D Modeling of Dynamic Recrystallization.” *Modelling and Simulation in Materials Science and Engineering* 21 (8): 085012. <https://doi.org/10.1088/0965-0393/21/8/085012>.
- . 2014. “Influence of Anisotropic Grain Boundary Properties on the Evolution of Grain Boundary Character Distribution during Grain Growth—a 2D Level Set Study.” *Modelling and Simulation in Materials Science and Engineering* 22 (8): 085005. <https://doi.org/10.1088/0965-0393/22/8/085005>.
- Hallberg, H., and V. V. Bulatov. 2019. “Modeling of Grain Growth under Fully Anisotropic Grain Boundary Energy.” <https://doi.org/10.1088/1361-651X/ab0c6c>.
- Harun, A., E. A. Holm, M. P. Clode, and M. A. Miodownik. 2006. “On Computer Simulation Methods to Model Zener Pinning.” *Acta Materialia* 54 (12): 3261–73. <https://doi.org/10.1016/j.actamat.2006.03.012>.
- Hassold, G.N., E.A. Holm, and D.J. Srolovitz. 1990. “Effects of Particle Size on Inhibited Grain Growth.” *Scripta Metallurgica et Materialia* 24 (1): 101–6. [https://doi.org/10.1016/0956-716X\(90\)90574-Z](https://doi.org/10.1016/0956-716X(90)90574-Z).
- He, D., N. N. Ekere, and L. Cai. 1999. “Computer Simulation of Random Packing of Unequal Particles.” *Physical Review E Statistical Physics Plasmas Fluids And Related Interdisciplinary Topics* 60 (6 Pt B): 7098–7104. <http://www.ncbi.nlm.nih.gov/pubmed/11970649>.
- Hillert, M. 1965. “On the Theory of Normal and Abnormal Grain Growth.” *Acta Metallurgica* 13 (3): 227–38. [https://doi.org/10.1016/0001-6160\(65\)90200-2](https://doi.org/10.1016/0001-6160(65)90200-2).

- Hitti, K, P Laure, T Coupez, L Silva, and M Bernacki. 2012. "Precise Generation of Complex Statistical Representative Volume Elements (RVEs) in a Finite Element Context." *Computational Materials Science* 61: 224–38.
- Humphreys, F. J., and M. Hatherly. 2004. *Recrystallization and Related Annealing Phenomena*. *Acta Metallurgica et Materialia*. Pergamon. <http://books.google.com/books?hl=en&lr=&id=52Gloa7HxGsC&oi=fnd&pg=PP2&dq=Recrystallization+and+related+phenomenon∓ots=LfyfeiKxkx&sig=8JFnaDx2VSUvwYvpW68gpXKyXDM>.
- Humphreys, J., G. S. Rohrer, and A. Rollett. 2017. "Computer Modeling and Simulation of Annealing." *Recrystallization and Related Annealing Phenomena*, January, 569–604. <https://doi.org/10.1016/B978-0-08-098235-9.00016-1>.
- Ilin, D.N., and M. Bernacki. 2016a. "A New Algorithm for Dense Ellipse Packing and Polygonal Structures Generation in Context of FEM or DEM." In *MATEC Web of Conferences*. Vol. 80. <https://doi.org/10.1051/mateconf/20168002004>.
- . 2016b. "Advancing Layer Algorithm of Dense Ellipse Packing for Generating Statistically Equivalent Polygonal Structures." *Granular Matter* 18 (3). <https://doi.org/10.1007/s10035-016-0646-9>.
- Imai, H., M. Iri, and K. Murota. 1985. "Voronoi Diagrams in the Laguerre Geometry and Its Applications." *SIAM Journal on Computing* 14: 93–105.
- Janssens, K. G. F. 2010. "An Introductory Review of Cellular Automata Modeling of Moving Grain Boundaries in Polycrystalline Materials." *Mathematics and Computers in Simulation* 80 (7): 1361–81. <https://doi.org/10.1016/j.matcom.2009.02.011>.
- Jin, Y., N. Bozzolo, A. D. Rollett, and M. Bernacki. 2015. "2D Finite Element Modeling of Misorientation Dependent Anisotropic Grain Growth in Polycrystalline Materials: Level Set versus Multi-Phase-Field Method." *Computational Materials Science* 104: 108–23. <https://doi.org/10.1016/j.commatsci.2015.03.012>.
- Jodrey, T. 1985. "Computer Simulation of Close Random Packing of Equal Spheres." *Physical Review A* 32 (4): 2347. <https://doi.org/10.1103/PhysRevA.32.2347>.
- Johnson, W., and R. Mehl. 1939. "Reaction Kinetics in Processes of Nucleation and Growth." *Trans. Am. Inst. Min. Metall. Eng.* 135: 416–58.
- Jones, M. W., J. A. Baerentzen, and M. Sramek. 2006. "3D Distance Fields: A Survey of Techniques and Applications." *IEEE Transactions on Visualization and Computer Graphics* 12 (4): 581–99. <https://doi.org/10.1109/TVCG.2006.56>.
- Kad, B. K., and P. M. Hazzledine. 1997. "Monte Carlo Simulations of Grain Growth and Zener Pinning." *Materials Science and Engineering: A* 238 (1): 70–77. [https://doi.org/10.1016/S0921-5093\(97\)00435-8](https://doi.org/10.1016/S0921-5093(97)00435-8).
- Kansal, A. R., S. Torquato, and F. H. Stillinger. 2002. "Computer Generation of Dense Polydisperse Sphere Packings." *The Journal of Chemical Physics* 117 (18): 8212. <https://doi.org/10.1063/1.1511510>.
- Kimmel, R., and J. A. Sethian. 1998. "Computing Geodesic Paths on Manifolds." *Proceedings of the National Academy of Sciences of the United States of America* 95 (15): 8431–35. <https://doi.org/10.1073/PNAS.95.15.8431>.
- Kolmogorov, A. N. 1937. "Statistical Theory of Crystallization of Metals." *Bull. Acad.*

- Sci. USSR Mat Ser.* 1 24: 355–59.
- Krill III, C.E., and L.-Q. Chen. 2002. “Computer Simulation of 3-D Grain Growth Using a Phase-Field Model.” *Acta Materialia* 50 (12): 3059–75. [https://doi.org/10.1016/S1359-6454\(02\)00084-8](https://doi.org/10.1016/S1359-6454(02)00084-8).
- Lochmann, K., L. Oger, and D. Stoyan. 2006. “Statistical Analysis of Random Sphere Packings with Variable Radius Distribution.” *Solid State Sciences* 8 (12): 1397–1413. <https://doi.org/10.1016/j.solidstatesciences.2006.07.011>.
- Logé, R., M. Bernacki, H. Resk, L. Delannay, H. Dignonnet, Y. Chastel, and T. Coupez. 2008. “Linking Plastic Deformation to Recrystallization in Metals Using Digital Microstructures.” *Philosophical Magazine* 88 (30–32): 3691–3712. <https://doi.org/10.1080/14786430802502575>.
- Logé, R., H. Resk, Z. Sun, L. Delannay, and M. Bernacki. 2010. “Modeling of Plastic Deformation and Recrystallization of Polycrystals Using Digital Microstructures and Adaptive Meshing Techniques.” *Steel Research International*. http://gateway.webofknowledge.com/gateway/Gateway.cgi?GWVersion=2&SrcAuth=ORCID&SrcApp=OrcidOrg&DestLinkType=FullRecord&DestApp=WO_S_CPL&KeyUT=WOS:000208594600351&KeyUID=WOS:000208594600351.
- Ludwig, W., A. King, P. Reischig, M. Herbig, E.M. Lauridsen, S. Schmidt, H. Proudhon, et al. 2009. “New Opportunities for 3D Materials Science of Polycrystalline Materials at the Micrometre Lengthscale by Combined Use of X-Ray Diffraction and X-Ray Imaging.” *Materials Science and Engineering: A* 524 (1–2): 69–76. <https://doi.org/10.1016/J.MSEA.2009.04.009>.
- Maire, L., J. Fausty, M. Bernacki, N. Bozzolo, P. De Micheli, and C. Moussa. 2018. “A New Topological Approach for the Mean Field Modeling of Dynamic Recrystallization.” *Materials and Design*. <https://doi.org/10.1016/j.matdes.2018.03.011>.
- Maire, L., C. Moussa, N. Bozzolo, and M. Bernacki. 2019. “Full Field and Mean Field Modeling of Dynamic Recrystallization in 304L Steel.” *To Appear*.
- Maire, L., B. Scholtes, C. Moussa, N. Bozzolo, D.P. Muñoz, A. Settefrati, and M. Bernacki. 2017. “Modeling of Dynamic and Post-Dynamic Recrystallization by Coupling a Full Field Approach to Phenomenological Laws.” *Materials and Design* 133. <https://doi.org/10.1016/j.matdes.2017.08.015>.
- Maire, L., B. Scholtes, C. Moussa, N. Bozzolo, D. Pino Muñoz, and M. Bernacki. 2016. “Improvement of 3D Mean Field Models for Capillarity-Driven Grain Growth Based on Full Field Simulations.” *Journal of Materials Science* 51 (24). <https://doi.org/10.1007/s10853-016-0309-6>.
- Mallick, A., and S. Vedantam. 2009. “Phase Field Study of the Effect of Grain Boundary Energy Anisotropy on Grain Growth.” *Computational Materials Science* 46 (1): 21–25. <https://doi.org/10.1016/J.COMMATSCI.2009.01.026>.
- Manohar, P. A., M. Ferry, and T. Chandra. 1998. “Five Decades of the Zener Equation.” *ISIJ International* 38 (9): 913–24. <https://doi.org/10.2355/isijinternational.38.913>.
- Merriman, B., J. K. Bence, and S. J. Osher. 1994. “Motion of Multiple Junctions: A Level Set Approach.” *Journal of Computational Physics* 112 (2): 334–63. <https://doi.org/10.1006/jcph.1994.1105>.

- Micheli, P. O. De, L. Maire, D. Cardinaux, C. Moussa, N. Bozzolo, and M. Bernacki. 2019. "DIGIMU ® : Full Field Recrystallization Simulations for Optimization of Multi-Pass Processes." In *ESAFORM 2019 Proceedings*.
- Micheli, P. O. De, L. Maire, C. Moussa, N. Bozzolo, and M. Bernacki. 2019. "DIGIMU ® : 2D and 3D Full Field Recrystallization Simulations with Coupled Micro - Macro Approaches." In *NEMU 2019 Proceedings*.
- Mießén, C., M. Liesenjohann, L.A. Barrales-Mora, L.S. Shvindlerman, and G. Gottstein. 2015. "An Advanced Level Set Approach to Grain Growth – Accounting for Grain Boundary Anisotropy and Finite Triple Junction Mobility." *Acta Materialia* 99 (October): 39–48. <https://doi.org/10.1016/J.ACTAMAT.2015.07.040>.
- Miyoshi, Eisuke, and Tomohiro Takaki. 2017. "Multi-Phase-Field Study of the Effects of Anisotropic Grain-Boundary Properties on Polycrystalline Grain Growth." *Journal of Crystal Growth* 474 (September): 160–65. <https://doi.org/10.1016/J.JCRYSGRO.2016.11.097>.
- Moelans, N., B. Blanpain, and P. Wollants. 2005. "A Phase Field Model for the Simulation of Grain Growth in Materials Containing Finely Dispersed Incoherent Second-Phase Particles." *Acta Materialia* 53 (6): 1771–81. <https://doi.org/10.1016/j.actamat.2004.12.026>.
- . 2006. "Phase Field Simulations of Grain Growth in Two-Dimensional Systems Containing Finely Dispersed Second-Phase Particles." *Acta Materialia* 54 (4): 1175–84. <https://doi.org/10.1016/J.ACTAMAT.2005.10.045>.
- Montheillet, F., O. Lurdos, and G. Damamme. 2009. "A Grain Scale Approach for Modeling Steady-State Discontinuous Dynamic Recrystallization." *Acta Materialia* 57 (5): 1602–12. <http://cat.inist.fr/?aModele=afficheN&cpsidt=21295741>.
- Morawiec, A. 2009. "Models of Uniformity for Grain Boundary Distributions." *Journal of Applied Crystallography* 42 (5): 783–92. <https://doi.org/10.1107/S0021889809025461>.
- Murgas, B., J. Fausty, N. Bozzolo, and M. Bernacki. 2019. "Effect of Heterogeneous Mobility during Grain Boundary Motion." In *Colloque "La Métallurgie, Quel Avenir!"*
- Olmsted, D. L. 2009. "A New Class of Metrics for the Macroscopic Crystallographic Space of Grain Boundaries." *Acta Materialia* 57 (9): 2793–99. <https://doi.org/10.1016/J.ACTAMAT.2009.02.030>.
- Osher, S., and J.A. Sethian. 1988. "Fronts Propagating with Curvature-Dependent Speed." *Journal of Computational Physics* 79 (1): 12–49.
- Phaneesh, K. R., A. Bhat, P. Mukherjee, and K. T. Kashyap. 2012. "On the Zener Limit of Grain Growth through 2D Monte Carlo Simulation." *Computational Materials Science* 58 (June): 188–91. <https://doi.org/10.1016/J.COMMATSCI.2012.02.013>.
- Piękoś, K., J. Tarasiuk, K. Wierzbanowski, and B. Bacroix. 2008. "Generalized Vertex Model of Recrystallization – Application to Polycrystalline Copper." *Computational Materials Science* 42 (4): 584–94. <https://doi.org/10.1016/j.commatsci.2007.09.014>.

- Piot, D., G. Smaghe, J. J. Jonas, C. Desrayaud, F. Montheillet, G. Perrin, A. Montouchet, and G. Kermouche. 2018. “A Semitopological Mean-Field Model of Discontinuous Dynamic Recrystallization: Toward a Correct and Rapid Prediction of Grain-Size Distribution.” *Journal of Materials Science*. <https://doi.org/10.1007/s10853-018-2137-3>.
- Polychronopoulou, D., N. Bozzolo, D. Pino Muñoz, J. Bruchon, M. Shakoob, Y. Millet, C. Dumont, I. Freiherr von Thüngen, R. Besnard, and M. Bernacki. 2017. “Introduction to the Level-Set Full Field Modeling of Laths Spheroidization Phenomenon in α/β Titanium Alloys.” *International Journal of Material Forming*. <https://doi.org/10.1007/s12289-017-1371-6>.
- Proudhon, H., J. Li, P. Reischig, N. Guéninchault, S. Forest, and W. Ludwig. 2016. “Coupling Diffraction Contrast Tomography with the Finite Element Method.” *Advanced Engineering Materials* 18 (6): 903–12. <https://doi.org/10.1002/adem.201500414>.
- Quey, R., P. R. Dawson, and F. Barbe. 2011. “Large-Scale 3D Random Polycrystals for the Finite Element Method: Generation, Meshing and Remeshing.” *Computer Methods in Applied Mechanics and Engineering* 200 (17–20): 1729–45. <https://doi.org/10.1016/j.cma.2011.01.002>.
- Quey, R., and L. Renversade. 2018. “Optimal Polyhedral Description of 3D Polycrystals: Method and Application to Statistical and Synchrotron X-Ray Diffraction Data.” *Computer Methods in Applied Mechanics and Engineering* 330 (March): 308–33. <https://doi.org/10.1016/J.CMA.2017.10.029>.
- Raabe, D. 2002. “Cellular Automata in Materials Science with Particular Reference to Recrystallization Simulation.” *Annual Review of Materials Research*. <https://doi.org/10.1146/annurev.matsci.32.090601.152855>.
- Radhakrishnan, B., G. Sarma, and T. Zacharia. 2008. “Monte Carlo Simulation of Deformation Substructure Evolution during Recrystallization*” 39 (12): 1639–45.
- Radhakrishnan, B., G.B. Sarma, and T. Zacharia. 1998. “Modeling the Kinetics and Microstructural Evolution during Static Recrystallization—Monte Carlo Simulation of Recrystallization.” *Acta Materialia* 46 (12): 4415–33. [https://doi.org/10.1016/S1359-6454\(98\)00077-9](https://doi.org/10.1016/S1359-6454(98)00077-9).
- Resk, H., L. Delannay, M. Bernacki, T. Coupez, and R. Logé. 2009. “Adaptive Mesh Refinement and Automatic Remeshing in Crystal Plasticity Finite Element Simulations.” *Modelling and Simulation in Materials Science and Engineering* 17 (7): 075012. <https://doi.org/10.1088/0965-0393/17/7/075012>.
- Rollett, A. D. 2004. “Modeling Polycrystalline Microstructures in 3D.” In *AIP Conference Proceedings*, 712:71–77. AIP. <https://doi.org/10.1063/1.1766503>.
- Rollett, A. D., and D. Raabe. 2001. “A Hybrid Model for Mesoscopic Simulation of Recrystallization.” *Computational Materials Science* 21 (1): 69–78. [https://doi.org/10.1016/S0927-0256\(00\)00216-0](https://doi.org/10.1016/S0927-0256(00)00216-0).
- Rollett, A. D., D. Saylor, J. Fridy, B. S. El-Dasher, A. Brahme, S.-B. Lee, C. Cornwell, and R. Noack. 2004. “Modeling Polycrystalline Microstructures in 3D.” In *AIP Conference Proceedings*, 712:71–77. AIP. <https://doi.org/10.1063/1.1766503>.
- Rollett, A.D., D.J. Srolovitz, R.D. Doherty, and M.P. Anderson. 1989. “Computer

- Simulation of Recrystallization in Non-Uniformly Deformed Metals.” *Acta Metallurgica* 37 (2): 627–39. [https://doi.org/10.1016/0001-6160\(89\)90247-2](https://doi.org/10.1016/0001-6160(89)90247-2).
- Scholtes, B. 2016. “Development of an Efficient Level Set Framework for the Full Field Modeling Recrystallization in 3D.” PSL Research University. <https://pastel.archives-ouvertes.fr/tel-01719664>.
- Scholtes, B., R. Boulais-Sinou, A. Settefrati, D. Pino Muñoz, I. Poitault, A. Montouchet, N. Bozzolo, and M. Bernacki. 2016. “3D Level Set Modeling of Static Recrystallization Considering Stored Energy Fields.” *Computational Materials Science* 122. <https://doi.org/10.1016/j.commatsci.2016.04.045>.
- Scholtes, B., D. Ilin, A. Settefrati, N. Bozzolo, A. Agnoli, and M. Bernacki. 2016. “Full Field Modeling of the Zener Pinning Phenomenon in a Level Set Framework - Discussion of Classical Limiting Mean Grain Size Equation.” In *Proceedings of the International Symposium on Superalloys*. Vol. 2016-Janua.
- Scholtes, B., M. Shakoor, A. Settefrati, P.-O. Bouchard, N. Bozzolo, and M. Bernacki. 2015. “New Finite Element Developments for the Full Field Modeling of Microstructural Evolutions Using the Level-Set Method.” *Computational Materials Science* 109. <https://doi.org/10.1016/j.commatsci.2015.07.042>.
- Sethian, J. A. 1996. “A Fast Marching Level Set Method for Monotonically Advancing Fronts.” *Proceedings of the National Academy of Sciences of the United States of America* 93 (4): 1591–95. <https://doi.org/10.1073/PNAS.93.4.1591>.
- Sethian, James A, and Alexander Vladimirsky. 2003. “Ordered Upwind Methods for Static Hamilton–Jacobi Equations: Theory and Algorithms *.” *Society* 41 (1): 325–63.
- Shakoor, M., M. Bernacki, and P.-O. Bouchard. 2015. “A New Body-Fitted Immersed Volume Method for the Modeling of Ductile Fracture at the Microscale: Analysis of Void Clusters and Stress State Effects on Coalescence.” *Engineering Fracture Mechanics* m. <https://doi.org/10.1016/j.engfracmech.2015.06.057>.
- Shakoor, M., B. Scholtes, P.-O. Bouchard, and M. Bernacki. 2015. “An Efficient and Parallel Level Set Reinitialization Method – Application to Micromechanics and Microstructural Evolutions.” *Applied Mathematical Modelling*. <https://doi.org/10.1016/j.apm.2015.03.014>.
- Shi, Y., and Y. Zhang. 2008. “Simulation of Random Packing of Spherical Particles with Different Size Distributions.” *Applied Physics A* 92 (3): 621–26. <https://doi.org/10.1007/s00339-008-4547-6>.
- Sieradzki, L., and L. Madej. 2013. “A Perceptive Comparison of the Cellular Automata and Monte Carlo Techniques in Application to Static Recrystallization Modeling in Polycrystalline Materials.” *Computational Materials Science* 67 (February): 156–73. <https://doi.org/10.1016/J.COMMATSCI.2012.08.047>.
- Smith, C. S. 1948. “Grains, Phases, and Interphases: An Interpretation of Microstructure.” *Trans. Metall. Soc. AIME, Vol. 175, p. 15-51 (1948)*. 175: 15–51. <http://adsabs.harvard.edu/abs/1948TrMS..175...15S>.
- Srolovitz, D. J., M. P. Anderson, G. S. Grest, and P. S. Sahni. 1984. “Computer Simulation of Grain Growth-III. Influence of a Particle Dispersion.” *Acta Metallurgica* 32 (9): 1429–38. [https://doi.org/10.1016/0001-6160\(84\)90089-0](https://doi.org/10.1016/0001-6160(84)90089-0).
- Sussman, M., P. Smereka, and S. Osher. 1994. “A Level Set Approach for Computing

- Solutions to Incompressible Two-Phase Flow.” *Journal of Computational Physics* 114 (1): 146–59. <https://doi.org/10.1006/JCPH.1994.1155>.
- Sutton, A. P., and R. W. Balluffi. 1995. *Interfaces in Crystalline Materials*. Clarendon Press. <https://global.oup.com/academic/product/interfaces-in-crystalline-materials-9780199211067?cc=fr&lang=en&>.
- Tonks, M. R., Y. Zhang, A. Butterfield, and X.-M. Bai. 2015. “Development of a Grain Boundary Pinning Model That Considers Particle Size Distribution Using the Phase Field Method.” *Modelling and Simulation in Materials Science and Engineering* 23 (4): 045009. <https://doi.org/10.1088/0965-0393/23/4/045009>.
- Villaret, F., B. Hary, Y. de Carlan, T. Baudin, R. Logé, L. Maire, and M. Bernacki. 2019. “Full Field Methodologies to Simulate Recrystallization in ODS Steels - Illustrations and Discussions.” *To Appear*.
- Wang, W., A. L. Helbert, F. Brisset, M. H. Mathon, and T. Baudin. 2014. “Monte Carlo Simulation of Primary Recrystallization and Annealing Twinning.” *Acta Materialia* 81 (December): 457–68. <https://doi.org/10.1016/J.ACTAMAT.2014.08.032>.
- Weygand, D., Y. Brechet, and J. Lépinoux. 2001. “A Vertex Simulation of Grain Growth in 2D and 3D.” *Advanced Engineering Materials* 3 (1–2): 67–71. [https://doi.org/10.1002/1527-2648\(200101\)3:1/2<67::AID-ADEM67>3.0.CO;2-P](https://doi.org/10.1002/1527-2648(200101)3:1/2<67::AID-ADEM67>3.0.CO;2-P).
- Xu, T., and M. Li. 2009. “Topological and Statistical Properties of a Constrained Voronoi Tessellation.” *Philosophical Magazine* 89 (4): 349–74. <https://doi.org/10.1080/14786430802647065>.
- Young, P. G., T. B. H Beresford-West, S. R. L. Coward, B. Notarberardino, B. Walker, and A. Abdul-Aziz. 2008. “An Efficient Approach to Converting Three-Dimensional Image Data into Highly Accurate Computational Models.” *Philosophical Transactions of the Royal Society A: Mathematical, Physical and Engineering Sciences* 366 (1878): 3155–73. <https://doi.org/10.1098/rsta.2008.0090>.
- Yu, Qi., M. Nosonovsky, and S. K. Esche. 2009. “Monte Carlo Simulation of Grain Growth of Single-Phase Systems with Anisotropic Boundary Energies.” *International Journal of Mechanical Sciences* 51 (6): 434–42. <https://doi.org/10.1016/j.ijmecsci.2009.03.011>.
- Zhang, L., A. D. Rollett, Ti. Bartel, D. Wu, and M. T. Lusk. 2012. “A Calibrated Monte Carlo Approach to Quantify the Impacts of Misorientation and Different Driving Forces on Texture Development.” *Acta Materialia* 60 (3): 1201–10. <https://doi.org/10.1016/j.actamat.2011.10.057>.
- Zhang, Y., C. Bajaj, and B.-S. Sohn. 2005. “3D Finite Element Meshing from Imaging Data.” *Computer Methods in Applied Mechanics and Engineering* 194 (48–49): 5083–5106. <https://doi.org/10.1016/j.cma.2004.11.026>.
- Zhao, H. K., T. Chan, B. Merriman, and S. Osher. 1996. “A Variational Level Set Approach to Multiphase Motion.” *Journal of Computational Physics* 127 (1): 179–95. <https://doi.org/10.1006/jcph.1996.0167>.
- Zouari, M., N. Bozzolo, and R. E. Loge. 2016. “Mean Field Modelling of Dynamic and Post-Dynamic Recrystallization during Hot Deformation of Inconel 718 in the

Absence of δ Phase Particles.” *Materials Science and Engineering A*.
<https://doi.org/10.1016/j.msea.2015.12.102>.